Environmental Pollution 215 (2016) 141–153

Contents lists available at ScienceDirect

Environmental Pollution

journal homepage: www.elsevier.com/locate/envpol

Correlating microbial community profiles with geochemical conditions in a watershed heavily contaminated by an antimony tailing pond☆

Enzong Xiao [a, b], Valdis Krumins [c], Song Tang [d], Tangfu Xiao [a, e, *], Zengping Ning [a], Xiaolong Lan [a, b], Weimin Sun [f, g, **]

[a] State Key Laboratory of Environmental Geochemistry, Chinese Academy of Sciences, Guiyang 550081, China
[b] University of Chinese Academy of Sciences, Beijing 100049, China
[c] Department of Environmental Sciences, Rutgers University, New Brunswick, NJ 08901, USA
[d] School of Environment and Sustainability, University of Saskatchewan, Saskatoon S7N5B3, Canada
[e] Innovation Center and Key Laboratory of Waters Safety & Protection in the Pearl River Delta, Ministry of Education, Guangzhou University, Guangzhou 510006, China
[f] Guangdong Institute of Eco-environment and Soil Sciences, Guangzhou 510650, China
[g] Department of Microbiology and Biochemistry, Rutgers University, New Brunswick, NJ 08901, USA

ARTICLE INFO

Article history:
Received 23 February 2016
Received in revised form
22 April 2016
Accepted 25 April 2016
Available online 13 May 2016

Keywords:
Antimony and arsenic co-contamination
Mine tailings
Microbial community
High-throughput sequencing

ABSTRACT

Mining activities have introduced various pollutants to surrounding aquatic and terrestrial environments, causing adverse impacts to the environment. Indigenous microbial communities are responsible for the biogeochemical cycling of pollutants in diverse environments, indicating the potential for bioremediation of such pollutants. Antimony (Sb) has been extensively mined in China and Sb contamination in mining areas has been frequently encountered. To date, however, the microbial composition and structure in response to Sb contamination has remained overlooked. Sb and As frequently co-occur in sulfide-rich ores, and co-contamination of Sb and As is observed in some mining areas. We characterized, for the first time, the microbial community profiles and their responses to Sb and As pollution from a watershed heavily contaminated by Sb tailing pond in Southwest China. The indigenous microbial communities were profiled by high-throughput sequencing from 16 sediment samples (535,390 valid reads). The comprehensive geochemical data (specifically, physical-chemical properties and different Sb and As extraction fractions) were obtained from river water and sediments at different depths as well. Canonical correspondence analysis (CCA) demonstrated that a suite of *in situ* geochemical and physical factors significantly structured the overall microbial community compositions. Further, we found significant correlations between individual phylotypes (bacterial genera) and the geochemical fractions of Sb and As by Spearman rank correlation. A number of taxonomic groups were positively correlated with the Sb and As extractable fractions and various Sb and As species in sediment, suggesting potential roles of these phylotypes in Sb biogeochemical cycling.

1. Introduction

Antimony (Sb) is a naturally occurring trace element and the ninth most mined element in the world (Courtin-Nomade et al., 2012). Sb and its compounds are widely used in semiconductors, flame retardants, and certain therapeutic agents (Filella et al., 2002; Vasquez et al., 2006). Sb is extensively used and/or generated by anthropogenic activities (e.g. mining and smelting activities, industry uses, incineration of waste, combustion of fossil fuels and spent ammunition), leading to significant releases of Sb compounds to the environment (Okkenhaug et al., 2011). Sb is considered carcinogenic on the inhalation route by the International Agency for Research on Cancer (IARC) (An and Kim, 2009) and presents as one of the priority pollutants of the US

☆ This paper has been recommended for acceptance by Klaus Kummerer.
* Corresponding author. 99 Lincheng Road West, Guiyang 550081, China.
** Corresponding author. 14 College Farm Road, New Brunswick, NJ 08901, USA.
E-mail addresses: xiaotangfu@vip.gyig.ac.cn (T. Xiao), swm@envsci.rutgers.edu (W. Sun).

http://dx.doi.org/10.1016/j.envpol.2016.04.087
0269-7491/

Environmental Protection Agency (USEPA, 1979) and the European Union (Communities, 1976). China is the largest Sb producer in the world with more than 114 Sb mines (He et al., 2012). During the Sb mining processes, tailings, consisting of low grade ore minerals, gangue, and other minerals are generated. The Sb tailing piles present a high risk of contamination to adjacent environments with Sb or other metal(loid)s, and in fact, contamination of soils, rivers, and aquifers has been reported (Lee et al., 2015; Okkenhaug et al., 2011). Human exposure to antimony is known to cause the liver, lung, and cardiovascular system diseases (Feng et al., 2013; Gebel, 1997). Elevated Sb concentrations were a suspected cause of morbidity of dermatitis and pneumoconiosis for the local residents living near the Xikuangshan (XKS) Sb mine in Hunan Province, China (He and Yang, 1999). Microbial transformations of Sb are promising approaches for remediation of Sb-contaminated environments by facilitating *in situ* immobilization and precipitation. However, limited studies have addressed biogeochemical cycling of Sb (Filella et al., 2002). Eight Sb(III)-oxidizing bacteria, falling within two subdivisions of *Proteobacteria*, were isolated from the vicinity of a Sb oxide-producing factory (Nguyen and Lee, 2015). A metagenomic approach revealed diversity of microbes with Sb and As metabolism genes from highly contaminated soil (Luo et al., 2014). In another study, the microbial communities in a Sb- and As-rich neutral mine drainage tailings are profiled. Diverse communities of microorganisms including typical As-resistant heterotrophic species as well as iron reducers and sulfur oxidizers were found in the heavily contaminated environment (Majzlan et al., 2010). Two bacterial strains, *Hydrogenophaga taeniospiralis* strain IDSBO-1 and *Variovorax paradoxus* strain IDSBO-4, which can oxidize Sb(III) using either oxygen or nitrate were isolated from contaminated mine sediments (Terry et al., 2015). Microbiological reduction of Sb(V) to Sb(III) was observed in anoxic sediments from a Sb- and As-contaminated mine site (Stibnite Mine) in central Idaho and an uncontaminated suburban lake (Searsville Lake) in California (Kulp et al., 2013). The effect of microbiological transformation of As and Sb on bioaccumulation potential has also been studied in a freshwater ecosystem affected by mine drainage. Biogenic products of microbiological As and Sb cycling in sediment mats presented a direct route of uptake (by ingestion) of metalloids to tadpoles (Dovick et al., 2015).

We have characterized the microbial communities in a watershed severely contaminated by Sb. In this previous study, only surface sediments were available due to the shallow (~3 cm) sediment layers on top of the rocky river bed (Sun et al., 2016) and thus oxidized environments prevailed in that study site. Therefore, the effect of redox conditions on microbial communities could not be studied. For this reason, we investigated a watershed downstream of a Sb tailings pile located in Dushan County, southwest China. This watershed is also heavily contaminated with Sb and As, but sediments in this location are deeper. More reduced environments with negative Eh in deeper sediments were observed in all sampling site, allowing us to characterize the microbial communities in reduced environments. The objectives of this study therefore were (i) to characterize the indigenous microbial communities in an Sb- and As-impacted aquatic environment with elevated Sb up to 17,000 mg/kg and As up to 1100 mg/kg in sediment, (ii) to investigate the impact of As and Sb pollution gradients on microbial assemblage, (iii) to gain new insight into Sb and As biogeochemical process and microbially-mediated Sb and As transformation in this contaminated river environment, and (iv) to reveal the relationships of microbial taxa with other geochemical factors.

2. Materials and methods

2.1. Site description

The study site is located in the Shen watershed (105°30′23″E, 25°31′28″N) in Dushan County of eastern Guizhou Province, Southwest China (Fig. 1). This watershed is located downstream of a Sb tailing pond and consists of two small rivers, Xiao River and Shen River. Xiao River is immediately downstream of the Sb tailing pond and receives underground drainage from the pond. Xiao River flows for about 3 km before joining the Shen River. A total of eight sampling sites (A, B, D, E, H, I, J, and K) downstream of the Sb tailing pond were selected for geochemical and microbial analysis. Sampling sites were divided into two zones according to which river they were sampled from. Sites A, B, D, E, and H are from the Xiao River (Zone 1), while sites I, J, and K are from the Shen River (Zone 2). Site A locates in the upstream of the tailing pond and was regarded as less Sb-contaminated site. Site H is downstream of a small dam in Xiao River.

2.2. Sampling and sample preparation

At each sampling site, water and sediment samples were

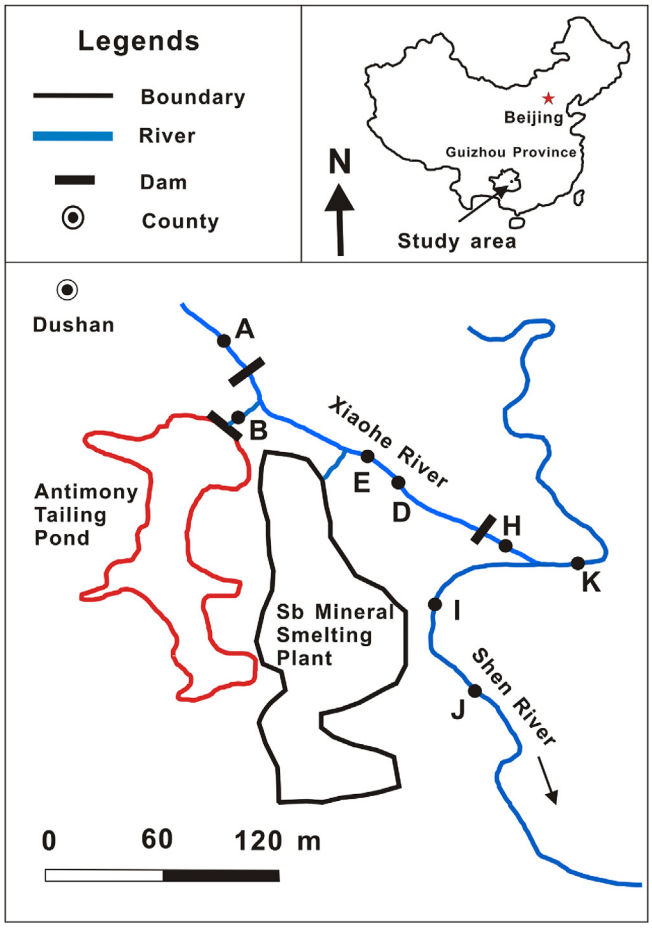

Fig. 1. Site location map of Sb-impacted Xiao and Shen Rivers, Southwest China. Annotated on the map are locations of the mine tailings pond and smeltery, as well as eight sampling sites (A–K) in the Shen watershed. Sediment samples are denoted as A1-K1 and A2-K2, water samples are denoted as AW-KW corresponding to their respective sampling sites.

collected. The water samples (AW-KW) were collected and immediately filtered through a 0.45 μm sterile membrane (Jinjing, Shanghai, China), and preserved with few drops of ultrapure 37% HCl (Kemiou, Tianjing, China) and stored at 4 °C for subsequent geochemical analysis. Water quality parameters including temperature (T), pH, dissolved oxygen (DO), electric conductivity (EC), and oxidation-reduction potentials (Eh) were measured onsite by a calibrated YSI Professional plus pH meter (YSI, Yellow Springs, OH, USA). The surface (0–10 cm) and deep (10–20 cm) sediment samples (Approximately 300 g each, denoted as samples A1-K1 and A2-K2, respectively) were collected using a columnar sediment sampler. The sediment samples were pooled and homogenized by stirring, placed in sterile 100 mL tubes. All sediment samples were frozen by ice bags in the field and immediately stored at the −20 °C freezer for geochemical analysis and −80 °C freezer for DNA extraction after transported to the lab. Sediment samples were freeze-dried at laboratory for 48 h and thoroughly ground using a mortar and pestle before passing through a 200-mesh sieve. Approximately 50 mg of the sieved sediment sample was digested using a heated acid mixture (15 mL of 15 M HNO_3 and 5 mL of 10 M HF) to determine total Sb and As. To measure anions in sediment, 2 g of dry sediment was mixed with 10 mL of distilled water, shaken for 5 min and left to equilibrate for 4 h. The supernatant was then centrifuged 3500×g for 15 min and filtered with a 0.45-μm filter membrane, and the filtrates were for anion determination.

2.3. Sequential extraction of sediment

A three-stage sequential extraction of Sb and As in sediment samples was performed in accordance with the modified procedures for As (Wenzel et al., 2001). We aim to measure three extractable fractions including the easily exchangeable (M_{exe}, M stands for Sb or As, hereafter), specifically-sorbed surface-bound (M_{srp}), and amorphous hydrous oxides of iron-aluminum (M_{amr}) fractions. Briefly, 1 g of dry sediment was placed in a 50 mL centrifugation tube. The M_{exe} was extracted through the addition of 10 mL 0.05 M $(NH_4)_2SO_4$ solution followed by agitation for 4 h. Next, the M_{srp} was extracted by shaking the residual sediment with 10 mL of 0.05 M $NH_4H_2PO_4$ for 16 h. Finally, a fraction containing M_{amr} was targeted by the addition of 10 mL of 0.2 M ammonium oxalate buffer (pH 3.0), followed by a 4 h reaction time with agitation in the dark. The residual fraction (M_{res}) was obtained by subtracting the above three extracted fractions from Sb_{tot}. All equipments were acid-washed and all reagents were analytical grade (Kemoiou, Tianjing, China). Extractions were performed at room temperature (~20 °C) and all shaking was done at 200 rpm. After each extraction stage, samples were centrifuged at 3000 rpm for 15 min and the supernatant was removed and analyzed by ICP-MS (Agilent, 7700x, California, USA).

2.4. Analysis of geochemical parameters

The concentrations of Sb and As were measured using inductively coupled plasma mass spectrometry (ICP-MS) (Agilent, 7700x, Santa Clara, CA, USA). Anions in water and sediment filtrates were measured by ion chromatography (Dionex, ICS-90, Sunnyvale, CA, USA). Total sulfur, soluble sulfur, total organic carbon (TOC), total nitrogen (TN), total hydrogen (TH), and total carbon (TC) in sediments were measured by an elemental analyzer (Elementar, Hanau, Germany) (Schumacher, 2002). Total Fe and Fe(II) were measured by a spectrophotography (UV-9000s, Shanghai METASH) with 1,10-phenanthroline at 510 nm (Tamura et al., 1974). Fe(III) was determined as the difference between total Fe and Fe(II). The redox species of Sb and As (III and V) were determined by HG-AFS (AFS-920, Beijing Jitian) with the method described by Gonzálvez et al. and Chen et al., respectively (Chen et al., 2014; Gonzálvez et al., 2009). The detection limit for Sb, calculated as the average of ten times the standard deviation of the ion counts obtained from the individual procedural reagent blanks (prepared in the same way as the sample decomposition), were 0.2 μg/L and 1 mg/kg for water and sediment samples, respectively, lower than the Sb concentrations in this study. The analytical precision was determined based on the standard quality control procedures using internationally certified reference materials (SLRS-5), internal standards (Rh at 500 μg/L), and duplicates, was better than ±10%. The standard reference material GBW07310 (Chinese National Standard) was used for analytical quality control (Ning et al., 2015). The average total Sb concentration of GBW07310 was 6.5 ± 0.8 mg/kg (n = 6), which is comparable to the certified value of 6.3 ± 0.9 mg/kg.

2.5. DNA extraction

The DNA was extracted from 250 mg samples using the MoBio Power Soil DNA extraction kit (MO BIO Laboratories, Carlsbad, CA, USA) following the manufacturer's instructions. DNA concentration and purity was checked by running the extracts on 1.2% agarose gels.

2.6. PCR amplification of 16S rRNA genes and high-throughput sequencing

The V4–V5 region of bacterial 16S-rRNA genes were amplified using the universal primers 515F (GTGCCAGCMGCCGCGGTAA) and 926R (CCGTCAATTCMTTTRAGTTT). These primers were chosen because of their high coverage of almost all phyla in conventional and metagenomic studies (Baker et al., 2003; Liu et al., 2008; Wang and Qian, 2009). The primers also contained the Illumina 5'overhang adapter sequences for two-step amplicon library building, following manufacturer's instructions for the overhang sequences. The initial PCR reactions were carried out in 25 μL reaction volumes with 1 μL DNA template, 250 μM dNTPs, 0.25 μM of each primer, 1X reaction buffer and 0.5U Phusion DNA Polymerase (New England Biolabs, USA). PCR conditions consisted of initial denaturation at 94 °C for 2 min, followed by 25 cycles of denaturation at 94 °C for 30 s, annealing at 56 °C for 30 s and extension at 72 °C for 30 s, with a final extension of 72 °C for 5 min. The Illumina Next era XT Index kit (Illumina Inc., San Diego, CA, USA) with dual 8-base barcodes were used for multiplexing. Eight cycle PCR reactions were used to incorporate two unique barcodes to either end of the 16S amplicons. Cycling conditions consisted of one cycle of 94 °C for 3 min, followed by eight cycles of 94 °C for 30 s, 56 °C for 30 s and 72 °C for 30 s, followed by a final extension cycle of 72 °C for 5 min. Prior to library pooling, the barcoded PCR products were purified using a DNA gel extraction kit (Axygen, China) and quantified using the Qubit dsDNA HS Assay Kit (Life Technologies, Carlsbad, CA, USA). The libraries were sequenced by 2 × 300 bp paired-end sequencing on the MiSeq platform using MiSeq v3 Reagent Kit (Illumina) at Tiny Gene Bio-Tech (Shanghai) Co., Ltd.

2.7. Bioinformatics and statistical analysis

All sequences were processed using Mothur (version 1.35.1) (Schloss et al., 2009). Sequences were sorted by barcode and filtered to remove ambiguous reads and any reads shorter than 200 bp or longer than 600 bp. The set of remaining sequences was simplified using the 'unique.seqs' command to generate a unique set of sequences, then aligned with the SILVA database of 16S rRNA sequences, version 119 (Pruesse et al., 2007). Chimeric sequences were filtered using the 'chimera. Uchime' command with default parameters. The candidate sequences were assigned to the

taxonomy with 'classify.seqs' command (Wang approach) with a confidence threshold of 80%. Any sequences aligning to eukaryota, chloroplasts or mitochondria were discarded, as well as unknown sequences. Then the distance matrix between the aligned sequences was generated by the 'dist.seqs' command. Finally, these sequences were clustered into operational taxonomic units (OTUs) at 97% sequence identity using the furthest neighbor method. Majority consensus taxonomy for each OTU was obtained by the 'classify.otu' command with default parameters. The reads were deposited into the NCBI short reads archive database under accession number of SRP069068.

The similarity of microbial communities among different sediment samples was determined using both weighted and unweighted UniFrac. A principal component analysis (PCA) based on weighted UniFrac distance was used to quantify differences in community composition. Alpha diversity (Shannon, Simpson, and Evenness) and richness (ACE and Chao1) (Ling et al., 2013) indices were determined for the OTUs as well. Linear discriminant analysis (LDA) effect size (LEfSe) (http://huttenhower.sph.harvard.edu/lefse/) was used to characterize microbial community features differentiating the heavily contaminated zones (Zone 1) from the moderately contaminated zones (Zone 2), as described previously (Ling et al., 2014; Segata et al., 2011). LEfSe uses the Kruskal-Wallis rank sum test to detect features with significantly different abundances between treatments (in this case, levels of contamination) and performs LDA to estimate the effect size of each feature with a normalized relative abundance matrix. All tests for significance were two-sided and p values < 0.05 were considered statistically significant. Canonical correspondence analysis (CCA, CANOCO 4.5 Microcomputer Power, Ithaca, NY) was used to measure the major physicochemical parameters that had the greatest influence on microbial community structure. CCA was done on abundant bacteria genera (relative abundance >1% in at least one sequencing library) and selected physicochemical parameters. 999 Monte Carlo permutation tests with manual forward selection were then performed to determine the significance of the environmental variables (Lepš and Šmilauer, 2003).

3. Results

3.1. Distribution of Sb and As in the watershed

The distribution of the aqueous Sb (Sb_{aq}) (Table 1), total Sb concentrations in the sediments (Sb_{tot}), and different Sb extractable fractions demonstrated zone-specific trends (Table 2). The Sb_{aq} concentrations were higher in Xiao River, ranging from 2691 (HW) to 7990 μg/L (BW), but decreased in Shen River, ranging from 42.4 (KW) to 157.3 (IW) μg/L, compared with the relatively 'pristine' sample site (AW), which had 38 μg/L aqueous Sb. Sb_{tot} in the sediments varied from 2624 to 17,453 mg/kg, while the concentrations of extractable Sb fractions were lower than Sb_{tot} (Table 2 and Fig. S1). Easily exchangeable Sb (Sb_{exe}) concentrations ranged from 28.58 (B1) to 87.36 mg/kg (E2) in Zone 1 and from 2.2 (K1) to 15.06 mg/kg (H1) in Zone 2. The sum of the two Sb fractions considered 'bioaccessible', Sb_{exe} and Sb_{srp}, accounted for 0.7% (A2) to 23.8% (I2) of Sb_{tot}, while the three Sb extractable fractions together only accounted for 1% (A2) to 32.5% (I1) of Sb_{tot} (Buanuam and Wennrich, 2010). The bioaccessible Sb fractions accounted for higher proportion of Sb_{tot} in Zone 2 (6%–23.8%) than Zone 1 (0.7%–5.4%) (Fig.S1). Moreover, the concentrations of Sb(III) and Sb(V) were measured in the pore water of the sediments. Sb(III) and Sb(V) fluctuated remarkably along the watershed, with the maximum concentration at E2 (Table 3). SEM-EDS analyses also showed that Sb was one of the major components in the mineralized structures of sediments (Fig. 2).

In addition to Sb, concentrations of As and its extractable fractions were measured as well. This watershed was also characterized as a high-As aqueous environment. The total As (As_{tot}) concentrations ranged from 64 (H2) to 1167.7 (A2) mg/kg in sediment, and 6.8–221.6 μg/L in the water. Similar to Sb, the bioaccessible As also constituted a small portion of total As (Table 2). As(III) and As(V) were also measured in the pore water of the sediments and were summarized in Table 4.

The aqueous pH along the watershed was greater than 7 at all sampling sites, indicating slightly alkaline environment (Table 1). The whole watershed demonstrated oxidized environments in the surface water with Eh greater than 100 mV in all sampling sites. In comparison, some sediments in this study exhibited reducing conditions and Eh values generally decreased with depth in the sediments (Table 4). Aqueous sulfate (SO_4^{2-}) concentrations were relatively higher in Zone 1 (222–1478 mg/L) than in Zone 2 (64.9–91.7 mg/L). Total Fe was relatively higher in the Xiao River than Shen River. In comparison, the measurement of total Fe and Fe(II) in pore water indicated that higher concentrations of Fe were observed in samples taken from Shen River. In addition, TN, TC, TOC, TH, and soluble sulfur in all sediment samples were summarized in Table 4. TC and TOC were generally higher in Zone 2, while total and soluble sulfur were higher in Zone 1.

3.2. Taxonomic profiles

After filtering the low quality reads, chimeras, and trimming the adapters, barcodes, and primers, there were 535,390 valid reads identified from the sixteen sediment samples through Illumina MiSeq platform, with the average sequence length of 420 bp (Table S1). The microbial community diversity at the phylum level was shown in Fig.S2. The rarefaction curves were shown in supplementary Fig. S3. *Proteobacteria* was the most abundant phylum in all samples, except I2 in which *Firmicutes* was the most abundant phylum. *Proteobacteria* accounted for 44.6% of the total valid reads in all samples. *Actinobacteria* accounted for 14.5% of the total valid reads and >20% of reads in samples H1 and H2.

Table 1
Chemical and physical parameters of river water samples from each site.

Sample	T (°C)	DO (mg/L)	EC (μS/cm)	pH	Eh (mv)	Cl^- (mg/L)	NO_3^- (mg/L)	SO_4^{2-} (mg/L)	Sb (μg/L)	As (μg/L)	Fe (mg/L)	Fe(II) (mg/L)
AW	20.1	6.6	1552	7.65	240.1	5.67 ± 0.06	0.87 ± 0.05	222.2 ± 1.4	38.2 ± 5.4	3.4 ± 0.5	11.0	N.D.
BW	20.6	3.2	4932	7.04	101.2	22.49 ± 0.5	0.7	1478 ± 9.5	7990 ± 388	221.6 ± 17.8	7.4	0.20
DW	25.7	2.9	2750	8.39	275.8	18.11 ± 11.6	9.81 ± 6.1	553.1 ± 5.1	3161 ± 139	87.6 ± 2.9	23.3	0.14
EW	28	4.9	2604	8.38	291.2	16.4 ± 10.5	9.67 ± 5.9	453.5 ± 1.4	3075 ± 95	61.5 ± 2.2	23.4	0.13
HW	24.8	6.2	2602	8.15	201.6	23.84 ± 0.1	12.36 ± 2.5	472.1 ± 4.7	2691 ± 27	135 ± 3.1	2.5	0.10
IW	21.5	6.2	1144	7.98	283.6	29.18 ± 0.2	21.90 ± 0.8	83.3 ± 0.1	157 ± 18.3	32.3 ± 16.4	3.6	0.11
JW	21.6	6.6	1133	8.01	282.8	29.45 ± 0.7	25.45 ± 3.2	91.7 ± 11.1	123 ± 2.3	11.8 ± 0.6	21.3	0.11
KW	21.6	7.6	1068	8.20	308.1	29.64 ± 0.6	23.81 ± 0.9	64.9 ± 0.8	42 ± 3.3	6.8 ± 0.5	10.3	0.14

N.D.: Not detected.

Table 2
Concentrations (mg/kg) of different Sb extractable fractions in 16 samples. Note that Sb extractable fractions were measured in triplicate.

Operationally defined phase	Total digest		Easily exchangeable		Specifically sorbed		Amorphous crystalline hydrous oxides of Fe and Al	
	Sb_{tot}	As_{tot}	Sb_{exe}	As_{exe}	Sb_{srp}	As_{srp}	Sb_{amr}	As_{amr}
A1	786 ± 136	935 ± 344	1.5 ± 0.1	0.1	5.7 ± 0.4	1.1	2.6 ± 0.1	0.4
A2	990 ± 463	1168 ± 528	2.2 ± 0.1	0.1	4.5 ± 3.8	1.0 ± 0.8	3.8 ± 0.3	0.7 ± 0.1
B1	17,453 ± 422	439 ± 0.8	28.6 ± 1.9	0.1	125.6 ± 6.8	26.7 ± 0.6	203 ± 6.9	9.7 ± 0.2
B2	2625 ± 33.7	69.5 ± 3.9	53.9 ± 4.1	0.2	88.1 ± 4.3	2.7 ± 0.1	91.8 ± 4.9	1.0 ± 0.1
D1	3240 ± 20.1	848 ± 44.9	29.3 ± 1.6	1.2	48.1 ± 1.3	57.0 ± 1.9	80.6 ± 2.3	24.8 ± 0.3
D2	8441 ± 234	686 ± 40.3	58.8 ± 3.4	0.4	75.3 ± 4.3	36.8 ± 1.1	297 ± 13.9	21.7
E1	3488 ± 82	331 ± 13.3	76.6 ± 7.3	0.3	72.4 ± 23.1	9.5 ± 0.4	81.6 ± 4.4	3.6 ± 0.3
E2	7299 ± 59.1	1106 ± 13.1	87.4 ± 5.4	0.6	87.6 ± 29.1	79.5 ± 0.8	2686 ± 19.4	40.7 ± 0.9
H1	273 ± 14	492 ± 19.1	15.1 ± 1.1	0.4	14.7 ± 0.7	5.1 ± 0.1	66.6 ± 2.9	3.2 ± 0.3
H2	164 ± 6.2	64.0 ± 1.8	6.6 ± 0.2	0.2	7.7 ± 0.4	3.3 ± 0.1	19.9 ± 11.4	1.8 ± 0.2
I1	80.8 ± 8.2	887 ± 70	4.8 ± 0.8	0.7	9.0 ± 0.4	2.3 ± 0.1	12.5 ± 10.1	1.6 ± 0.1
I2	87.6 ± 3.1	490 ± 15.3	14.7 ± 0.8	0.2	6.2 ± 0.3	1.9 ± 0.1	7.4 ± 0.4	1
J1	318 ± 257	381 ± 4.1	9.0 ± 0.4	1.6	10.3 ± 0.5	4.3 ± 0.1	14.1 ± 0.5	2.3 ± 0.1
J2	100 ± 1.6	281 ± 6.1	2.9 ± 0.1	0.2	6.4 ± 0.4	1.3	5.0 ± 0.3	0.7
K1	100 ± 1.5	500 ± 17.3	2.2 ± 0.1	0.2	7.8 ± 0.4	3.5 ± 0.1	5.4 ± 0.2	1.9 ± 0.1
K2	76.1 ± 5.3	358 ± 9.6	2.7 ± 0.2	0.1	5.7 ± 0.3	2.4	3.9 ± 0.2	1.4 ± 0.1

A1-K1 = 0–10 cm depth and A2-K2 – 10–20 cm.

Table 3
Chemical parameters of pore water of the river sediment samples from each site.

Sample	Eh (mv)	Total As (μg/L)	As-III (μg/L)	Total Sb (μg/L)	Sb-III (μg/L)	Total Fe (mg/L)	Fe-II (mg/L)
A1	191.2 ± 8.5	55.83 ± 5.59	17.73 ± 1.97	21.27 ± 1.60	10.64 ± 2.25	N.D.	N.D.
A2	148.7 ± 4.0	66.67 ± 14.62	23.16 ± 1.75	843.25 ± 52.58	411.03 ± 24.47	N.D.	N.D.
B1	46.5 ± 1.8	72.19 ± 16.26	28.35 ± 1.11	1158.65 ± 110.87	583.52 ± 52.66	6.4	5.9
B2	−15.5 ± 1.8	82.60 ± 8.96	56.56 ± 1.46	1252.86 ± 84.14	702.92 ± 52.40	N.D.	N.D.
D1	74.3 ± 2.5	298.58 ± 3.82	240.14 ± 8.58	625.84 ± 37.81	320.03 ± 22.22	N.D.	N.D.
D2	−114.6 ± 4.5	424.21 ± 4.76	369.69 ± 12.13	469.99 ± 28.20	248.54 ± 24.78	1.1	0.8
E1	−55.7 ± 0.7	131.83 ± 24.19	107.04 ± 0.34	1493.01 ± 123.42	934.72 ± 91.40	N.D.	N.D.
E2	N.D.	120.29 ± 61.53	90.19 ± 34.04	3057.90 ± 151.98	2051.32 ± 201.58	N.D.	N.D.
H1	−92.8 ± 4.2	288.70 ± 3.86	207.23 ± 7.35	354.69 ± 19.56	214.29 ± 16.94	6.2	4.1
H2	N.D.	181.12 ± 6.13	151.54 ± 0.26	953.75 ± 57.21	680.24 ± 59.10	2.7	2.4
I1	−41.0 ± 4.2	88.04 ± 1.39	41.97 ± 1.65	560.90 ± 20.53	286.91 ± 7.10	9.6	9.6
I2	−44.3 ± 5.7	98.95 ± 4.89	72.96 ± 8.16	122.74 ± 6.96	56.36 ± 5.11	5.8	4.6
J1	23.3 ± 3.6	298.62 ± 24.76	236.47 ± 0.97	1535.74 ± 166.25	856.31 ± 21.49	12.7	12.4
J2	−85.3 ± 3.5	108.40 ± 14.01	80.16 ± 2.02	66.84 ± 0.35	54.21 ± 4.36	6.8	4.3
K1	−49.0 ± 0.7	83.46 ± 7.60	41.53 ± 6.34	15.59 ± 1.70	9.30 ± 0.96	5.1	2.2
K2	−100.4 ± 1.98	96.61 ± 6.91	49.48 ± 2.65	22.98 ± 1.17	11.98 ± 0.07	5.2	3.4

N.D.: Not detected. A1-K1 = 0–10 cm depth and A2-K2 – 10–20 cm.

Bacteroidetes (9.2% of total valid reads) and *Firmicutes* (7.1%) were the third and fourth most abundant phyla, respectively. Interestingly, *Firmicutes* was more abundant in bottom layer samples than their upper layer counterparts. The relative abundances of other abundant phyla including *Chloroflexi*, *Nitrospirae*, and *Cyanobacteria* were summarized in Table S2 and Fig.S2.

Further comparison of the dominant phyla down to the genus level was conducted to reveal the microbial community response to *in situ* geochemical conditions (Fig. 3). Various genera were enriched in different samples. For instance, *Demequina* exhibited high abundances in H1, H2, I1, J1, and J2. More specially, this genus was dominant in I1 (38.2%) and J1 (19.8%). *Cloacibacterium* was abundant in H1 (8.2%) and H2 (7.2%). *Chryseobacterium* was also abundant in H1 (8.2%) and H2 (12.4%). *Ferribacterium* was abundant in K1 (6.4%) and K2 (4%). *Desulfurivibrio* occurred at high abundance in B2 (8.7%). *Thiobacillus* demonstrated relative higher abundances at D2 (4.2%). The PCA analysis elucidated the differences between the 16 microbial communities (97% OTU sequence similarity) and indicated that the microbial communities from Zone 1 (A1, A2, B1, B2, D1, D2, E1, and E2) were clustered, while those from Zone 2 were distantly related to each other (Fig.S4).

3.3. Microbial communities corresponds to fractionated Sb in sediment

To identify the specific bacterial taxa associated with different levels of Sb contamination, we compared the microbial communities in Zone 1 (heavily Sb-contaminated areas) and Zone 2 (moderate Sb-contaminated areas) using linear discriminant analysis (LDA) effect size (LEfSe). A cladogram representative of the structure of the microbial communities and their predominant bacteria was shown in Fig. 4. Only taxa with LDA values higher than 2 were shown for clarity. At the phylum and sub-phylum level, delta-*Proteobacteria*, epsilon-*Proteobacteria*, *Acidobacteria*, and *Chlorobi* were enriched in heavily contaminated samples (red legend) with LDA value higher than 2. At the family level, *Nitrospiraceae*, *Syntrophobacterales*, *Myxococcales*, *Desulfuromonadales*, *Desulfobacterales*, *Nitrosomonadaceae*, *Hydrogenophilaceae*, and *Nitrospiraceae* were enriched in the heavily contaminated zone while *Flavobacteriales* and *Rhodobacteraceae* were prevalent in moderately contaminated zone. Four genera including *Desulfurivibrio*, *Thiobacillus*, *Silanimonas*, and *Nitrospira* had higher LDA values in Zone 1 while only one genus (*Gemmobacter*) had higher LDA value in Zone 2 (green legend).

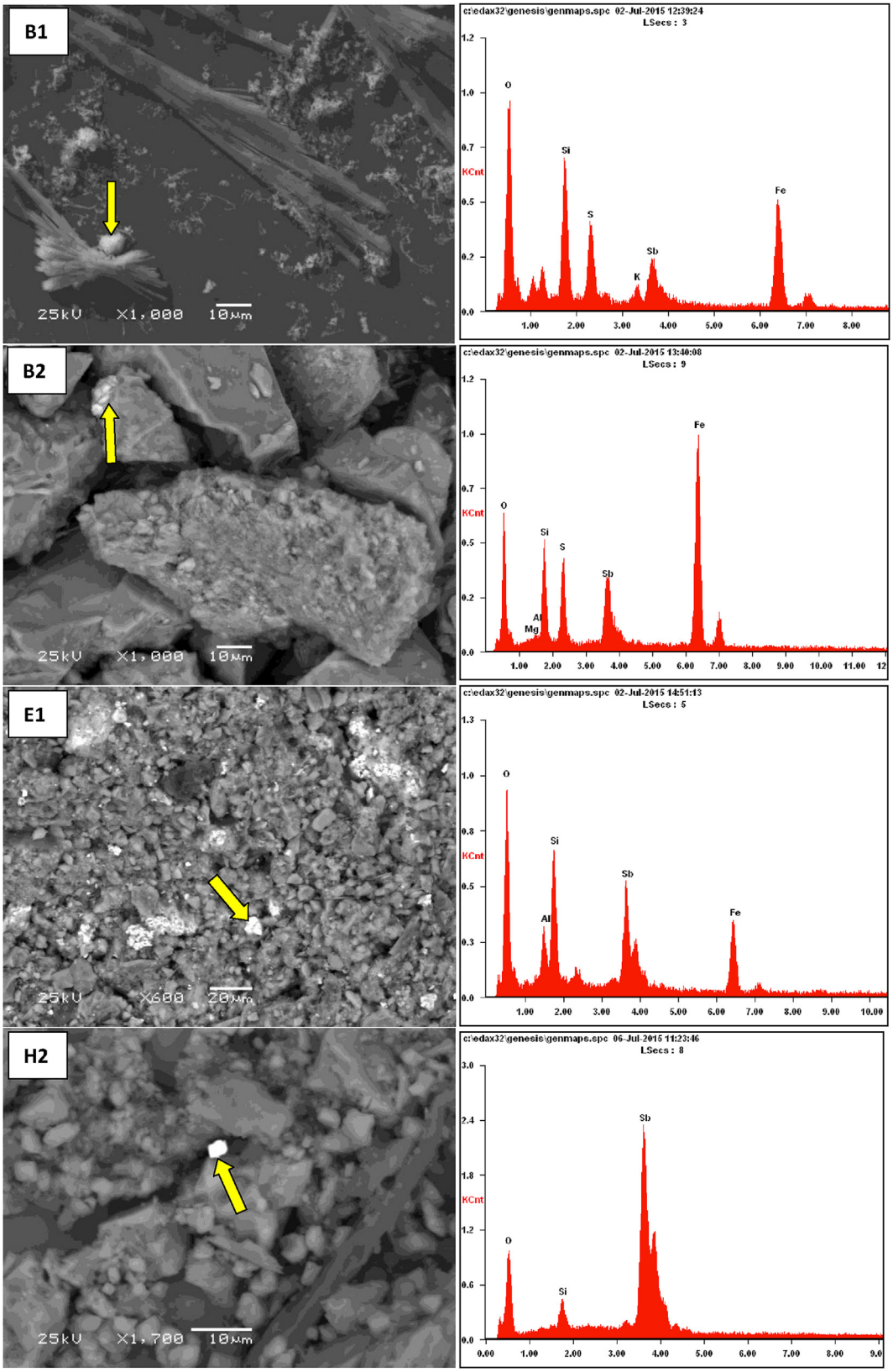

Fig. 2. Representative SEM images (left panel) and the corresponding EDX spectra (right panel) of the sediment samples. Sampling sites are labeled on top left of each panel. The arrows point to the exactly area for the EDS analysis.

Given the similar chemical structure and property of Sb and As (Byrd, 1990), Spearman rank correlations were determined between bacterial taxa and various forms of Sb and As including the two redox species (III and V) of Sb and As and the fractionated Sb

Table 4
Chemical parameters of the river sediment samples from each site.

Sample	Total N (%)	Total C (%)	Organic C (%)	Total H (%)	Total S (%)	Soluble S (%)	Total Fe (mg/Kg)	Cl^- (mg/L)	SO_4^{2-} (mg/L)
A1	0.03	0.4	0.2	0.3	0.5	0.1	22.4	2.0 ± 0.4	23.6 ± 10.3
A2	0.04	0.5	0.2	0.3	0.9	0.5	26.5	0.5 ± 0.02	38.3 ± 0.4
B1	0.05	0.6	0.2	0.4	0.9	0.4	61.7	5.0 ± 0.04	620 ± 61.2
B2	0.03	0.4	0.1	0.2	0.7	0.2	6.1	2.9 ± 0.3	405.7 ± 20.4
D1	0.1	3.1	1.8	0.8	6.6	4.4	49.9	7.8 ± 0.6	142.9 ± 20.4
D2	0.1	3.5	2.8	0.7	5.1	0.5	68.5	4.4 ± 0.9	480 ± 53.6
E1	0.05	2.6	1.6	0.4	2.4	N.D.	49.8	4.8 ± 0.3	439.2 ± 9.7
E2	0.1	3.5	1.7	0.9	4.9	3.2	57.0	11.2 ± 0.5	450.6 ± 5.1
H1	0.09	14.2	3.6	0.5	2.3	1.7	3.1	4.8 ± 0.4	59.4 ± 14.5
H2	0.09	14.9	4.4	0.6	2.1	0.5	3.9	6.0 ± 0.4	22.6 ± 5
I1	0.2	16.5	6.7	0.9	2.6	1.1	4.4	6.2 ± 1.6	65.9 ± 0.3
I2	0.1	15.5	6.1	0.9	2.3	1.2	4.2	5.5 ± 0.4	52.1 ± 45.2
J1	0.3	15.1	6.5	1.1	1.5	0.4	11.1	4.3 ± 1.1	19.7 ± 3.5
J2	0.2	17.5	8.3	1.1	2.1	0.9	4.4	4.7 ± 0.04	36.1 ± 18
K1	0.3	7.1	4.1	0.9	1.8	0.5	33.9	10.0 ± 0.3	422.2 ± 22.8
K2	0.3	6.6	3.6	0.9	0.9	N.D.	33.6	7.1 ± 0.04	503.3 ± 45.5

N.D.: Not detected, A1-K1 = 0–10 cm depth and A2-K2 – 10–20 cm.

and As. *Desulfurivibrio* was positively correlated with Sb in all the three extractable fractions as well as Sb_{tot}, Sb(III) and Sb(V) ($p < 0.01$, Fig. 5). *Thiobacillus* ($p < 0.01$) and *Desulfuromonas* ($p < 0.05$) were positively correlated with Sb_{tot}, while *Dechloromonas*, *Bacteroides*, *Saccharofermentans*, and *Propionicimonas* were negatively correlated with Sb_{tot} ($p < 0.05$). *Ferribacterium* ($p < 0.05$) was negatively correlated with Sb(III) and Sb(V). Three genera (*Demequina*, *Gemmobacter*, *Actinotalea*, and *Microbacterium*) were positively correlated with As_{exe}, while *Paludibacter* and *Prolixibacter* were negatively correlated with As_{srp} and As_{amr} ($p < 0.05$). As(V) was negatively correlated with a number of genera including *Desulfobulbus*, *Opitutus*, *Erysipelothrix*, *Paludibacter*, *Bacteroides*, *Treponema*, *Fusibacter*, and *Leptothrix*.

3.4. Relationship between microbial community and the geochemical conditions

Canonical correspondence analysis (CCA) was performed to discern possible linkages between the microbial communities and geochemical parameters in sediments (Fig. 6). SO_4^{2-}, TC, total N (TN), total Fe, and TOC were also strongly linked to bacterial community compositions (Fig. 6A). SO_4^{2-} was positively correlated with microbial communities from Zone 1 except H1 and H2. The relatively low magnitude of TS vectors indicated that these environmental factors were not as strongly correlated to community composition as other tested factors. CCA axis 1 was positively correlated with sulfate and total Fe, but was negatively correlated with total N, TOC, and TC (Fig. 6A). CCA axis 2 was positively correlated with TC, TOC, and TN, but was negatively correlated with total Fe in sediments.

The fractionated Sb in various extractable fractions, including Sb_{tot}, Sb_{exe}, Sb_{srp}, and Sb_{amp} as well as Sb(III) and Sb(V), were strongly correlated to community composition as indicated by the magnitude of their corresponding vectors, while the effect of As fractions and As(III) and As(V) was weaker (Fig. 6B). Additionally, the overall microbial communities in Zone 1 except for those from H1 and H2 (red dots) were positively correlated with the concentrations of fractionated Sb and As (except As_{exe}), while the microbial communities from Zone 2 (green dots) were negatively correlated with the fractionated Sb and As. The Sb_{exe} and Sb_{srp} were more important to structure the microbial community than other forms of Sb.

4. Discussion

4.1. Sb in the watershed

We estimate the total Sb and As loading in the streambed to be 1500 kg and 36 kg, respectively, from the tailing pond. This watershed was characterized by elevated Sb and As concentrations both in water and sediment, especially at Xiao River which is right downstream of the Sb tailing pond. The sediments of this watershed were characterized as having elevated Sb concentration, as high as 17,000 mg/kg; much higher than the Chinese background value (0.8–3.0 mg/kg) and sediment concentrations in the Yangtze River system (0.50–2.70 mg/kg). These concentrations are also much higher than those found in other Sb mining areas considered heavily contaminated, such as the Xikuangshan Sb mine (149 mg/kg) and Yata Au mining area (1163 mg/kg) (He et al., 2012). The Sb_{aq} concentrations were lower in Shen River mainly due to dilution by uncontaminated tributaries. The control site A demonstrated low concentration of Sb_{aq} but relative high concentrations of Sb_{tot}, partially due to the high background of Sb and/or dry/wet decompositions from the tailing dust and smelting site (Ning et al., 2015).

In Zone 1, the contents of Sb_{tot} were relatively higher than those from Zone 2 except H1 and H2. Although sample site H was located in Xiao River, this site demonstrated more similarity with downstream Shen River. This may be explained by the fact that H is far from the upstream sampling sites (B-E) and located at the downstream of a small dam, therefore, the water flows over this site but the Sb-rich sediments were trapped by the dam, resulting in the deposition of Sb before site H. This may also explained the relatively high concentration of Sb_{aq} but lower Sb_{tot} in H1 and H2. All the sediment samples in Zone 2 demonstrated relative lower Sb_{tot} than those in Zone 1 (except H1 and H2), suggesting the effect of dilution of uncontaminated water and deposition of Sb_{tot} upstream (in Xiao River) reduced the Sb input in the downstream river.

In the current study, sequential extractions were performed to determine the fractionated Sb and As in sediments. The Sb_{exe} and Sb_{srp}, are considered to be bioaccessible, while the Sb_{amr} and crystalline iron and aluminum oxide-bonding Sb (not measured in this study) are considered poorly bioaccessible (Buanuam and Wennrich, 2010; Savonina et al., 2012). The bioaccessible Sb fractions accounted for a relatively higher proportion of Sb_{tot} in Zone 2 and sites H1 and H2 in Zone 1 (Fig. S1). Thus, more poorly bioaccessible Sb precipitates close to the source, while more

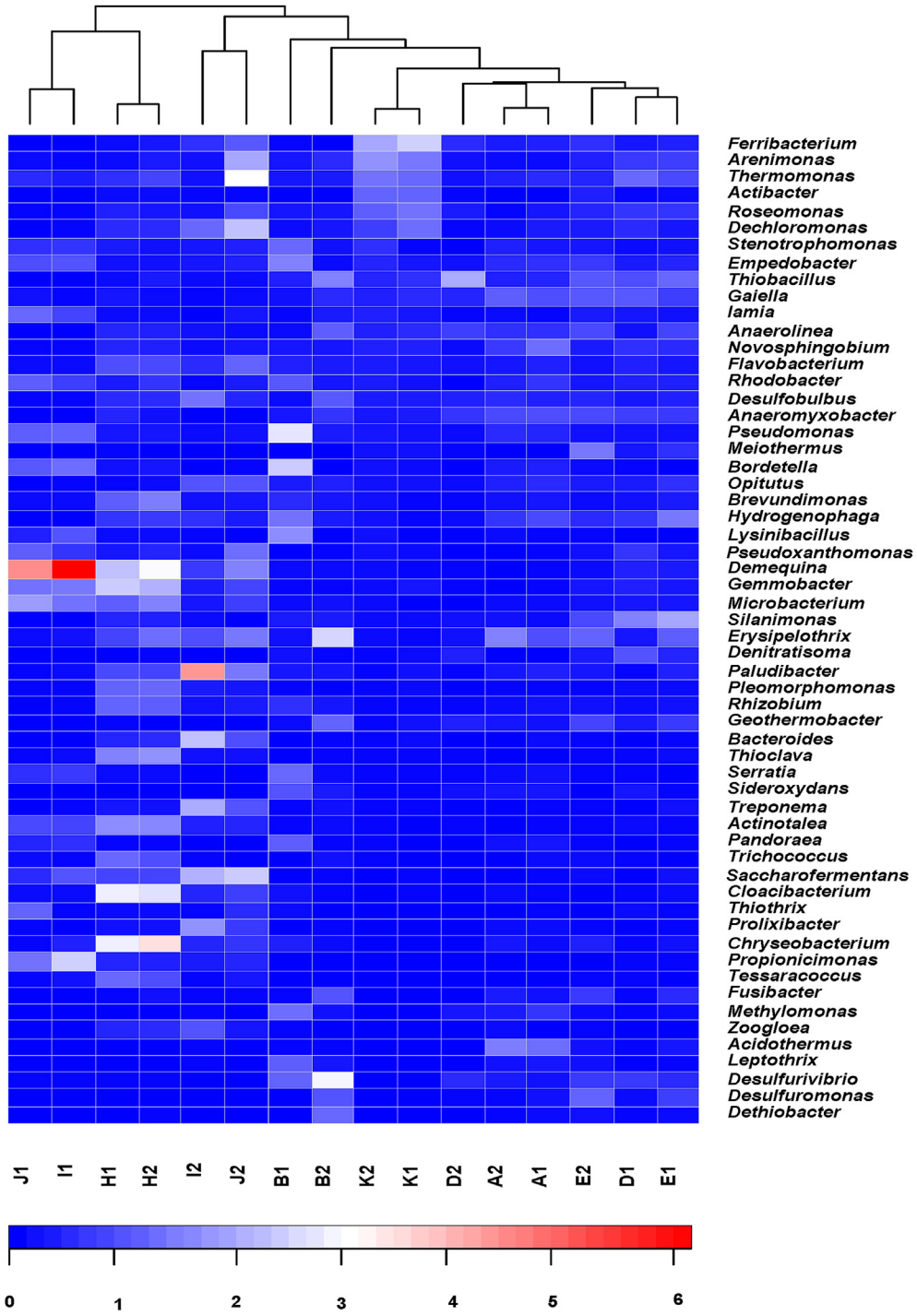

Fig. 3. Heatmap of the distribution of abundant genera with relative abundances >1% in at least one sample The relative percentage values for the microbial genera are indicated by hue.

bioaccessible Sb are precipitated downstream. The overall low bioaccessibility of Sb in the watershed is in accordance with previous studies showing low levels of soluble or bioaccessible Sb (Baroni et al., 2000; Flynn et al., 2003; Gál et al., 2007), suggesting that Sb is relatively immobile in the oxidized environment. The elevated concentrations of As both in the water and sediments indicated a co-contamination of Sb and As. One of the notable findings is that concentrations of Sb(III) and As(III) were elevated relative to Sb(V) and As(V) in some downstream samples where Eh was negative. We propose that the higher Sb(III) and As(III) may partially due to the microbially-mediated Sb and As cycling.

4.2. Relationship between Sb-contaminated environments with bacterial taxa

Although a large portion of the Sb and As were associated with immobile Sb and As phases, various Sb and As fractions still affected the community compositions from the overall microbial

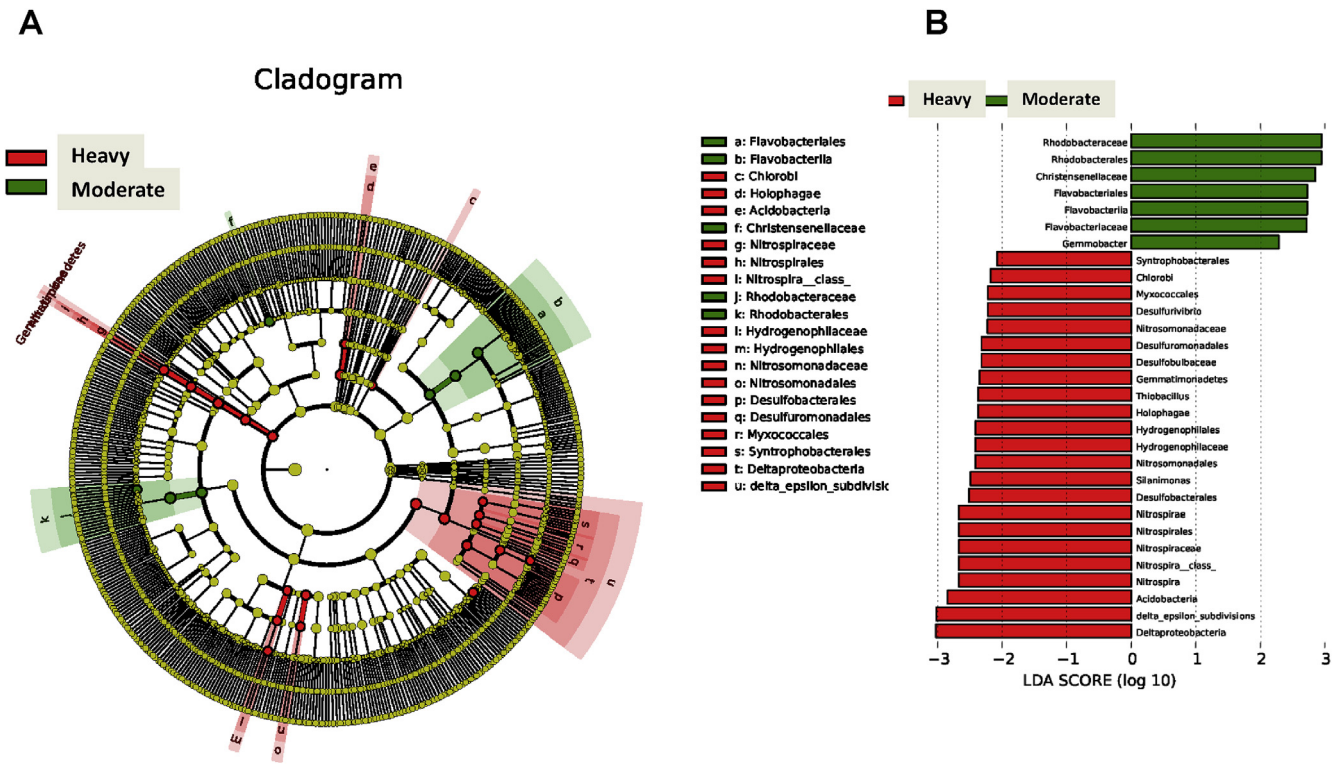

Fig. 4. LEfSe identified the most differentially abundant taxon between heavily contaminated area (red legend) and moderately contaminated area (green legend). (A) Taxonomic cladogram obtained from LEfSe analysis of 16S rRNA sequences (relative abundance > 0.5%). Small circles and shading with different colors in the diagram represent the abundance of those taxa in the respective treatment group. (Red) taxa enriched in heavily contaminated area; (Green) taxa enriched in moderately contaminated area. Yellow circles represent non-significant differences in abundance between heavily contaminated and moderate contaminated groups. The brightness of each dot is proportional to its effect size. (B) Taxa enriched in moderately zone are indicated with a positive LDA score (green), and taxa enriched in heavily zone have a negative score (red). Only taxa meeting an LDA significant threshold 2 are shown. (For interpretation of the references to colour in this figure legend, the reader is referred to the web version of this article.)

communities to the individual bacterial taxa based on the CCA, LEfSe, and Spearman rank correlations. CCA indicated that the fractionated Sb in sediments had significant correlations with the overall microbial communities, especially these from Zone 1. Therefore, it is reasonable to propose that the microbial communities could be governed by various Sb fractions in the watershed. The LEfSe confirmed that the microbial communities were shaped in part by Sb levels. Several bacterial taxonomic groups containing sulfate reducing bacteria (SRB) such as *Desulfobacterales* (order) to *Desulfurivibrio* (genus), *Desulfuromonadales* (order), and *Syntrophobacterales* (order) had higher LDA scores in the heavily Sb contaminated area, suggesting the tolerance of SRB to elevated Sb concentrations in reduced contaminated river sediments. The relative abundance of SRB in this study was much higher than in our previous work (Sun et al., 2016), which may reflect the fact that several samples in the current study came from the reduced environments, while most sample locations in the previous study were oxic.

Further, Spearman rank correlation test provided correlations between bacterial taxa and specific Sb and As species. It is noteworthy that *Desulfurivibrio* was significantly correlated with all tested Sb forms, suggesting a positive link between this genus with Sb. *Desulfurivibrio* was enriched in B1(1.4%) and B2 (8.7%) and demonstrated relative higher abundances in D1, and D2.In addition to SO_4^{2-}, *Desulfurivibrio* spp. are metabolically versatile and able to utilize other electron acceptors, including some metals (metalloids) such as uranium (U) (Lovley and Phillips, 1992), technetium (Tc) (Lloyd et al., 1999), chromium (Cr) (Lovley and Phillips, 1994), and selenium (Se) (Tucker et al., 1998). However, to our knowledge, *Desulfurivibrio* has never been associated with Sb biotransformation. It is reported that *Desulfurivibrio alkaliphilus* AHT 2 demonstrated 94% sequence similarity with Strain MLMS-1, which is able to grow lithoautotrophically with sulfide as electron donor and As(VI) as acceptor (Hoeft et al., 2004; Sorokin et al., 2008). Given the similar chemical structure of As and Sb, we could not exclude the potential role of *Desulfurivibrio* spp. in enzymatic Sb reduction.

We found that *Thiobacillus* is another genus positively correlated with Sb_{tot} ($p < 0.01$). *Thiobacillus* contains species that are aerobic disulfide-oxidizing species, which can use reduced SO_4^{2-} and Fe as sole energy sources (Temple and Colmer, 1951; Waksman and Joffe, 1922). Some *Thiobacillus* species also contain As resistance genes (Butcher et al., 2000) and show tolerance to As, As(III), and As(V) (Collinet and Morin, 1990). More interestingly, *Thiobacillus ferrooxidans* was reported to be able to oxidize stibnite (Sb_2S_3) and may oxidize sulfide in stibnite (Torma and Gabra, 1977). Although it is still not clear whether *Thiobacillus* is able to oxidize Sb(III), *Thiobacillus*-related bacteria may be able to resist and survive under the high Sb environments based on our results. While genus *Demequina* demonstrated very high abundances at Zone 2, especially in I1 (38.2%) and J1 (19.8%), and overall was positively correlated with As_{exe} ($p < 0.05$), our current understanding of this genus is very limited. *Demequina* spp. have been isolated from high Arctic permafrost soil (Finster et al., 2009), sea sediment (Hamada et al., 2013), marine environments (Ue et al., 2011), and a tidal flat (Park et al., 2015). Further research into the role of *Demequina* in contaminated environments is suggested.

Anaeromyxobacter was positively correlated with both Sb_{tot} and As_{tot}. *Anaeromyxobacter* sp. strain PSR-1 was isolated from As contaminated soil and identified as As(V)-reducing bacteria (Kudo

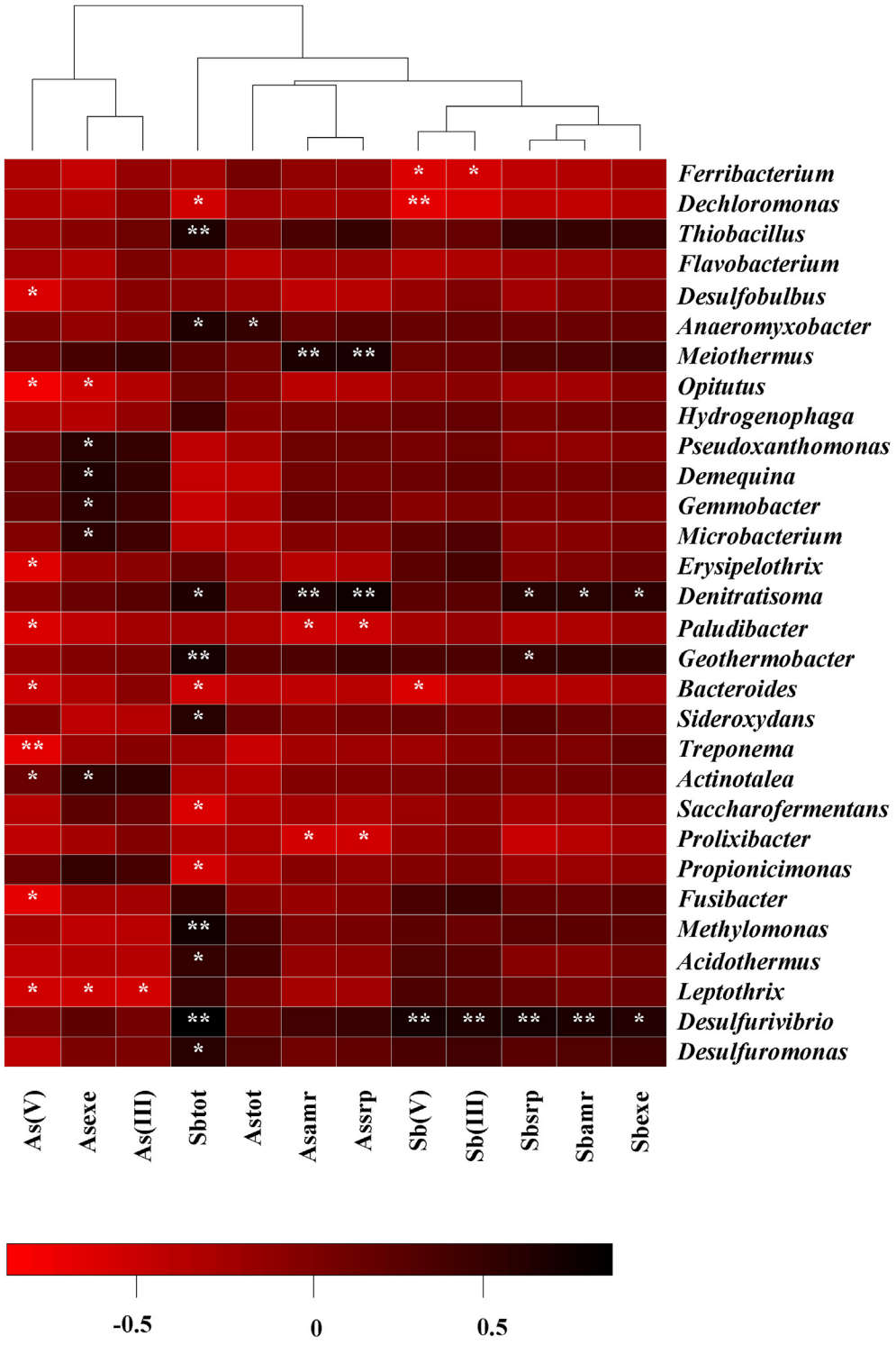

Fig. 5. Heat maps of Spearman's rank correlations coefficients and cluster analysis between the different Sb forms and the relative abundance of bacterial genera with relative abundances >1% in at least one sample. The correlation coefficients are indicated by hue. *, significant correlations ($p < 0.05$); **, significant correlations ($p < 0.01$). Abbreviations: As_{tot} (total As in sediment); Sb_{tot} (total Sb in sediment); Sb_{exe} (easily exchangeable forms of Sb); Sb_{srp} (specifically sorbed forms of Sb); Sb_{amr} (amorphous hydrous oxides of Fe and Al). As_{exe} (easily exchangeable forms of As); As_{srp} (specifically sorbed forms of As); As_{amr} (amorphous hydrous oxides of Fe and Al).

et al., 2013). Its draft genome contained three distinct As resistance gene clusters (ars operons) (Tonomura et al., 2015). In addition, *Anaeromyxobacter dehalogenans* strain 2CP-C can reduce a wide diversity of electron acceptors such as Fe(III), nitrate, nitrite, fumarate, oxygen, and U(VI) (Wu et al., 2006). These observations indicate the metabolic versatility of *Anaeromyxobacter* spp. toward various electron acceptors, indicating their potential role in the current study to reduce the As(V), or Sb(V). However, significant correlations between *Anaeromyxobacter* and As(V) and Sb(V) were not observed in this study. Dynamic microbial communities were

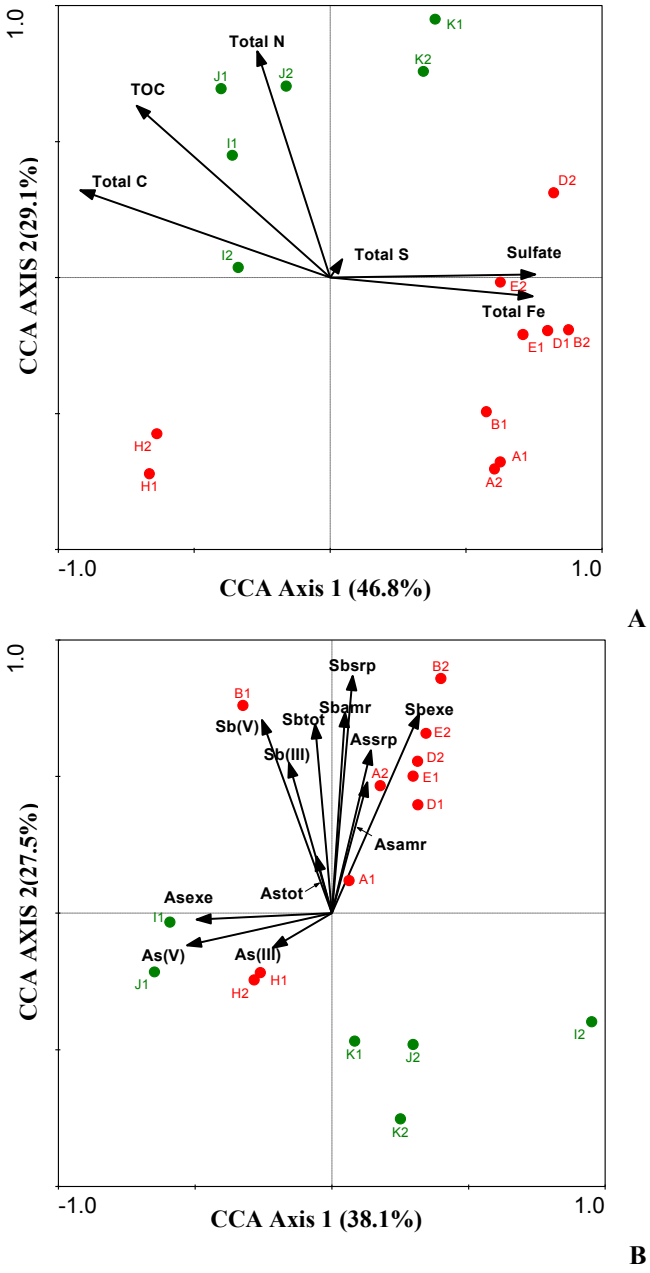

Fig. 6. Canonical correspondence analysis (CCA) of 16S rRNA gene data and the geochemical parameters (A) and Sb- and As-related fractions (B). A symbol's position in relation to a vector head indicates the correlation between the community and the environmental factors. The length of a vector reflects the relative importance of those environmental factors in discriminating the overall microbial community within one library (Zhang et al., 2008). Abbreviations: Astot (total As in sediment); Sbtot (total Sb in sediment); Sbexe (easily exchangeable forms of Sb); Sbsrp (specifically sorbed forms of Sb); Sbamr (amorphous hydrous oxides of Fe and Al); Sb(III) (Sb(III) in pore water of sediments); Sb(V) (Sb(V) in pore water of sediments); Asexe (easily exchangeable forms of As); Assrp (specifically sorbed forms of As); Asamr (amorphous hydrous oxides of Fe and Al); As(III) (As(III) in pore water of sediments); As(V) (As(V) in pore water of sediments); TC(total carbon); TOC (total organic carbon); Red dots represent sample locations with moderate contamination and green dots represent heavily contaminated samples. (For interpretation of the references to colour in this figure legend, the reader is referred to the web version of this article.)

observed in the present extremely contaminated study site and a number of taxonomic groups were significantly correlated with various forms of Sb and As, suggesting microorganism possible role in Sb and As cycling. Such biogeochemical cycling holds great potential for bioremediation. For instance, microorganisms may oxidize more toxic Sb(III) and As(III) to less toxic Sb(V) and As(V), respectively (Filella et al., 2009; Hamamura et al., 2013). The sulfate reduction by SRB generates sulfide as the reaction products. The sulfide in turn could react with Sb and As, resulting in the precipitation of insoluble metal sulfides that could be easily recovered and reused in further processes (Johnson and Hallberg, 2005). In addition, it is known that Sb and As species can be adsorbed by Fe-oxyhydroxide (Ashley et al., 2003). Such co-precipitation may lead to the immobilization of Sb and As from the aquatic environments. Therefore, investigation of microbial community structure and response of keystone taxa will help us facilitate the management and bioremediation of similar contaminated sites.

4.3. Correlations between other environmental data and bacterial communities

CCA analysis indicated strong effects of other geochemical parameters on the overall microbial communities. SO_4^{2-}, which has been identified as a primary environmental parameters in shaping microbial communities (Sun et al., 2015a), emerged as one of the most significant factors for structuring the bacterial community in the current study. In this study, the microbial communities of surface sediments and deeper samples from each sampling site were analyzed, facilitating comparison of the aerobic environments (upper layer) with anaerobic or facultative habitats (bottom layer) in microbial physiological groups (e.g. sulfate reducing bacteria). SO_4^{2-} concentrations influenced the overall bacterial communities by controlling the distribution of SRB. SRB were most abundant in samples with a high concentration of SO_4^{2-}. For example, *Desulfurivibrio*, *Desulfuromonas*, and *Desulfobulbus* were more abundant at Zone 1 which had relatively high SO_4^{2-} concentrations. Furthermore, we could not exclude the possibility of these SRB in Sb biotransformation because SRB can transform a wide variety of metal(loid)s (Barton et al., 2015; Sun et al., 2016). Fe was one of the metal(loid)s substantially shaping the overall microbial communities (Fig. 6A). Elevated Fe may foster the growth of Fe-metabolizing bacteria, especially in acidic Fe-rich environments such as acid mine drainage (Baker and Banfield, 2003; Sun et al., 2015c) and circumneutral groundwater Fe seeps (Blöthe and Roden, 2009; Roden et al., 2012). Fe was not particularly high across the site, but Fe_{tot} was elevated at sample locations K1 and K2. These two sites also demonstrated high relative abundances of *Ferribacterium*, a genus which contains Fe(III)-reducing bacteria (Cummings et al., 1999). Fe(II)-oxidizing bacteria, such as *Acidiferrobacter* and *Ferritrophicum*, were also detected in the sediments (Hallberg et al., 2011; Weiss et al., 2007). Thus, we propose a Fe cycling may exist in the watershed along with the Sb and As cycling.

TOC and TC are recognized as important for shaping the microbial community structure in various natural environments (Biegert et al., 1996; Cookson et al., 2005; Drenovsky et al., 2004; Li et al., 2014) and we also found TOC and TC significantly linked to microbial communities in this study. The allocation and composition of TOC and TC may change the distribution of heterotrophic microorganisms, such as *Dechloromonas*, *Anaerolinea*, *Polaromonas*, and *Thauera*, which have been reported to be able to degrade a number of organic matters (Coates et al., 2001; Sun and Cupples, 2012; Sun et al., 2015b, 2014, 2010). Further investigation of the types and amounts of carbon inputs to this system could help to explain the variability in microbial community composition.

5. Conclusions

In summary, a watershed heavily contaminated by Sb mine tailings provides an excellent opportunity to study the interaction

between Sb and microbial communities. Sb contamination has a profound impact on the prokaryotic microbial communities based on statistical analysis. Specifically, all forms of Sb (Sb_{tot}, Sb(III), Sb(V), Sb_{exe}, Sb_{srp}, and Sb_{amr}) and geochemical components (TC, TOC, and SO_4^{2-}) have an effect on structuring the overall microbial communities. Different taxonomic groups were enriched in heavily contaminated zone and moderately contaminated zone. A number of microbial phylotypes including *Desulfurivibrio*, *Anaeromyxobacter*, and *Thiobacillus* were positively correlated with different fractions of Sb and As, suggesting Sb and As tolerance or some role in Sb and As cycling. The current study will enhance our understanding of microbially-mediated Sb interaction and our ability to predict metabolisms of uncultured microbes in similar Sb-contaminated areas, which will in turn contribute to bioremediation of Sb-related contamination.

Acknowledgement

This research was funded by the Public Welfare Foundation of the Ministry of Water Resources of China (201501011), the National Natural Science Foundation of China (41103080, 41173028), the Opening Fund of the State Key Laboratory of Environmental Geochemistry (SKLEG2015907), and Guangdong Academy of Sciences (REN [2015] 20).

Appendix A. Supplementary data

Supplementary data related to this article can be found at http://dx.doi.org/10.1016/j.envpol.2016.04.087.

References

An, Y.J., Kim, M., 2009. Effect of antimony on the microbial growth and the activities of soil enzymes. Chemosphere 74, 654–663.
Ashley, P., Craw, D., Graham, B., Chappell, D., 2003. Environmental mobility of antimony around mesothermal stibnite deposits, New South Wales, Australia and southern New Zealand. J. Geochem. Expl. 77, 1–14.
Baker, B.J., Banfield, J.F., 2003. Microbial communities in acid mine drainage. FEMS Microbiol. Ecol. 44, 139–152.
Baker, G.C., Smith, J.J., Cowan, D.A., 2003. Review and re-analysis of domain-specific 16S primers. J. Microbiol. Methods. 55, 541–555.
Baroni, F., Boscagli, A., Protano, G., Riccobono, F., 2000. Antimony accumulation in *Achillea ageratum, Plantago lanceolata and Silene vulgaris* growing in an old Sb-mining area. Environ. Pollut. 109, 347–352.
Barton, L.L., Tomei-Torres, F.A., Xu, H., Zocco, T., 2015. Metabolism of metals and metalloids by the sulfate-reducing bacteria. In: Bacteria-metal Interactions. Springer, Switzerland, pp. 57–83.
Biegert, T., Fuchs, G., Heider, J., 1996. Evidence that anaerobic oxidation of toluene in the denitrifying bacterium*Thauera aromatica* is initiated by formation of benzylsuccinate from toluene and fumarate. Eur. J. Biochem. 238, 661–668.
Blöthe, M., Roden, E.E., 2009. Microbial iron redox cycling in a circumneutral-pH groundwater seep. Appl. Environ. Microbiol. 75, 468–473.
Buanuam, J., Wennrich, R., 2010. Dynamic flow-through sequential extraction for assessment of fractional transformation and inter-element associations of arsenic in stabilized soil and sludge. J. Hazard. Mater. 184, 849–854.
Butcher, B.G., Deane, S.M., Rawlings, D.E., 2000. The chromosomal arsenic resistance genes of *Thiobacillus ferrooxidans* have an unusual arrangement and confer increased arsenic and antimony resistance to *Escherichia coli*. Appl. Environ. Microbiol. 66, 1826–1833.
Byrd, J.T., 1990. Comparative geochemistries of arsenic and antimony in rivers and estuaries. Sci. Total. Environ. 97, 301–314.
Chen, M.L., Ma, L.Y., Chen, X.W., 2014. New procedures for arsenic speciation: a review. Talanta 125, 78–86.
Coates, J.D., Chakraborty, R., Lack, J.G., O'Connor, S.M., Cole, K.A., Bender, K.S., Achenbach, L.A., 2001. Anaerobic benzene oxidation coupled to nitrate reduction in pure culture by two strains of *Dechloromonas*. Nature 411, 1039–1043.
Collinet, M.-N., Morin, D., 1990. Characterization of arsenopyrite oxidizing *Thiobacillus*. Tolerance to arsenite, arsenate, ferrous and ferric iron. Ant. Leeuw 57, 237–244.
Cookson, W.R., Abaye, D.A., Marschner, P., Murphy, D.V., Stockdale, E.A., Goulding, K.W., 2005. The contribution of soil organic matter fractions to carbon and nitrogen mineralization and microbial community size and structure. Soil Biol. Biochem. 37, 1726–1737.
Courtin-Nomade, A., Rakotoarisoa, O., Bril, H., Grybos, M., Forestier, L., Foucher, F., Kunz, M., 2012. Weathering of Sb-rich mining and smelting residues: insight in solid speciation and soil bacteria toxicity. Chem. Erde. – Geochem. 72, 29–39.
Cummings, D.E., Caccavo Jr., F., Spring, S., Rosenzweig, R.F., 1999. Ferribacterium limneticum, gen. nov., sp. nov., an Fe (III)-reducing microorganism isolated from mining-impacted freshwater lake sediments. Arch. Microbiol. 171, 183–188.
Dovick, M.A., Kulp, T.R., Arkle, R.S., Pilliod, D.S., 2015. Bioaccumulation trends of arsenic and antimony in a freshwater ecosystem affected by mine drainage. Environ. Chem. 13, 149–159.
Drenovsky, R., Vo, D., Graham, K., Scow, K., 2004. Soil water content and organic carbon availability are major determinants of soil microbial community composition. Microb. Ecol. 48, 424–430.
Feng, R., Wei, C., Tu, S., Ding, Y., Wang, R., Guo, J., 2013. The uptake and detoxification of antimony by plants: a review. Environ. Exp. Bot. 96, 28–34.
Filella, M., Belzile, N., Chen, Y.-W., 2002. Antimony in the environment: a review focused on natural waters I. Occur. Earth Sci. Rev. 57, 125–176.
Filella, M., Williams, P.A., Belzile, N., 2009. Antimony in the environment: knowns and unknowns. Environ. Chem. 6, 95–105.
Finster, K.W., Herbert, R.A., Kjeldsen, K.U., Schumann, P., Lomstein, B.A., 2009. *Demequina lutea sp. nov.*, isolated from a high Arctic permafrost soil. Int. J. Syst. Evol. Microbiol. 59, 649–653.
Flynn, H.C., Meharg, A.A., Bowyer, P.K., Paton, G.I., 2003. Antimony bioavailability in mine soils. Environ. Pollut. 124, 293–100.
Gál, J., Hursthouse, A., Cuthbert, S., 2007. Bioavailability of arsenic and antimony in soils from an abandoned mining area, Glendinning (SW Scotland). J. Environ. Sci. Heal. A 42, 1263–1274.
Gebel, T., 1997. Arsenic and antimony: comparative approach on mechanistic toxicology. Chem. Biol. Interact. 107, 131–144.
Gonzálvez, A., Llorens, A., Cervera, M.L., Armenta, S., de la Guardia, M., 2009. Non-chromatographic speciation of inorganic arsenic in mushrooms by hydride generation atomic fluorescence spectrometry. Food. Chem. 115, 360–364.
Hallberg, K.B., Hedrich, S., Johnson, D.B., 2011. Acidiferrobacter thiooxydans, gen. nov. sp. nov.; an acidophilic, thermo-tolerant, facultatively anaerobic iron-and sulfur-oxidizer of the family Ectothiorhodospiraceae. Extremophiles 15, 271–279.
Hamada, M., Tamura, T., Yamamura, H., Suzuki, K.-I., Hayakawa, M., 2013. *Demequina flava sp. nov.* and *Demequina sediminicola sp. nov.*, isolated from sea sediment. Int. J. Syst. Evol. Microbiol. 63, 249–253.
Hamamura, N., Fukushima, K., Itai, T., 2013. Identification of antimony- and arsenic-oxidizing bacteria associated with antimony mine tailing. Microbes Environ. 28, 257–263.
He, M., Yang, J., 1999. Effects of different forms of antimony on rice during the period of germination and growth and antimony concentration in rice tissue. Sci. Total. Environ. 243–244, 149–155.
He, M., Wang, X., Wu, F., Fu, Z., 2012. Antimony pollution in China. Sci. Total. Environ. 421–422, 41–50.
Hoeft, S.E., Kulp, T.R., Stolz, J.F., Hollibaugh, J.T., Oremland, R.S., 2004. Dissimilatory arsenate reduction with sulfide as electron donor: experiments with Mono lake water and isolation of strain MLMS-1, a chemoautotrophic arsenate respirer. Appl. Environ. Microbiol. 70, 2741–2747.
Johnson, D.B., Hallberg, K.B., 2005. Acid mine drainage remediation options: a review. Sci. Total. Environ. 338, 3–14.
Kudo, K., Yamaguchi, N., Makino, T., Ohtsuka, T., Kimura, K., Dong, D.T., Amachi, S., 2013. Release of arsenic from soil by a novel dissimilatory arsenate- reducing bacterium, *Anaeromyxobacter sp. strain PSR-1*. Appl. Environ. Microbiol. 79, 4635–4642.
Kulp, T.R., Miller, L.G., Braiotta, F., Webb, S.M., Kocar, B.D., Blum, J.S., Oremland, R.S., 2013. Microbiological reduction of Sb(V) in anoxic freshwater sediments. Environ. Sci. Technol. 48, 218–226.
Lee, E., Han, Y., Park, J., Hong, J., Silva, R.A., Kim, S., Kim, H., 2015. Bioleaching of arsenic from highly contaminated mine tailings using *Acidithiobacillus thiooxidans*. J. Environ. Manag. 147, 124–131.
Lepš, J., Šmilauer, P., 2003. Multivariate Analysis of Ecological Data Using CANOCO. Cambridge University press, UK, pp. 1–282.
Li, J., Sun, W., Wang, S., Sun, Z., Lin, S., Peng, X., 2014. Bacteria diversity, distribution and insight into their role in S and Fe biogeochemical cycling during black shale weathering. Environ. Microbiol. 16, 3533–3547.
Ling, Z., Liu, X., Luo, Y., Yuan, L., Nelson, K.E., Wang, Y., Xiang, C., Li, L., 2013. Pyrosequencing analysis of the human microbiota of healthy Chinese undergraduates. BMC Genom. 14, 390.
Ling, Z., Liu, X., Jia, X., Cheng, Y., Luo, Y., Yuan, L., Wang, Y., Zhao, C., Guo, S., Li, L., 2014. Impacts of infection with different toxigenic *Clostridium difficile* strains on faecal microbiota in children. Sci. Rep. 4, 7485–7495.
Liu, Z., DeSantis, T.Z., Andersen, G.L., Knight, R., 2008. Accurate taxonomy assignments from 16S rRNA sequences produced by highly parallel pyrosequencers. Nucleic Acids Res. 36, e120.
Lloyd, J., Ridley, J., Khizniak, T., Lyalikova, N., Macaskie, L., 1999. Reduction of technetium by *Desulfovibrio desulfuricans*: biocatalyst characterization and use in a flowthrough bioreactor. Appl. Environ. Microbiol. 65, 2691–2696.
Lovley, D.R., Phillips, E.J., 1992. Reduction of uranium by *Desulfovibrio desulfuricans*. Appl. Environ. Microbiol. 58, 850–856.
Lovley, D.R., Phillips, E.J., 1994. Reduction of chromate by *Desulfovibrio vulgaris* and its *c3 cytochrome*. Appl. Environ. Microbiol. 60, 726–728.
Luo, J., Bai, Y., Liang, J., Qu, J., 2014. Metagenomic approach reveals variation of microbes with arsenic and antimony metabolism genes from highly contaminated soil. PLoS One. 9, 10–19.
Majzlan, J., Lalinska, B., Chovan, M., Blass, U., Brecht, B., Gottlicher, J., Steininger, R.,

Hug, K., Ziegler, S., Gescher, J., 2010. A mineralogical, geochemical, and microbiogical assessment of the antimony- and arsenic-rich neutral mine drainage tailings near Pezinok, Slovakia. Am. Miner. 96, 1–13.
Nguyen, V.K., Lee, J.-U., 2015. Antimony-oxidizing bacteria isolated from antimony-contaminated sediment–a phylogenetic study. Geomicrobiol. J. 32, 50–58.
Ning, Z., Xiao, T., Xiao, E., 2015. Antimony in the soil-plant system in an Sb mining/smelting area of southwest China. Int. J. Phytoremediat. 17, 1081–1089.
Okkenhaug, G., Zhu, Y.G., Luo, L., Lei, M., Li, X., Mulder, J., 2011. Distribution, speciation and availability of antimony (Sb) in soils and terrestrial plants from an active Sb mining area. Environ. Pollut. 159, 2427–2434.
Park, S., Jung, Y.-T., Won, S.-M., Lee, J.-S., Yoon, J.-H., 2015. *Demequina activiva sp. nov.*, isolated from a tidal flat. Int. J. Syst. Evol. Microbiol. 65, 2042–2047.
Pruesse, E., Quast, C., Knittel, K., Fuchs, B.M., Ludwig, W., Peplies, J., Glockner, F.O., 2007. SILVA: a comprehensive online resource for quality checked and aligned ribosomal RNA sequence data compatible with ARB. Nucleic Acids Res. 35, 7188–7196.
R Roden, E.E., McBeth, J.M., Blöthe, M., Percak-Dennett, E.M., Fleming, E.J., Holyoke, R.R., Luther III, G.W., Emerson, D., Schieber, J., 2012. The microbial ferrous wheel in a neutral pH groundwater seep. Front. Microbiol. 3, 172.
Savonina, E.Y., Fedotov, P., Wennrich, R., 2012. Fractionation of Sb and As in soil and sludge samples using different continuous-flow extraction techniques. Anal. Bioanal. Chem. 403, 1441–1449.
Schloss, P.D., Westcott, S.L., Ryabin, T., Hall, J.R., Hartmann, M., Hollister, E.B., Lesniewski, R.A., Oakley, B.B., Parks, D.H., Robinson, C.J., Sahl, J.W., Stres, B., Thallinger, G.G., Van Horn, D.J., Weber, C.F., 2009. Introducing mothur: open-source, platform-independent, community-supported software for describing and comparing microbial communities. Appl. Environ. Microbiol. 75, 7537–7541.
Schumacher, B.A., 2002. Methods for the Determination of Total Organic Carbon (TOC) in Soils and Sediments. Ecological Risk Assessment Support Center, pp. 1–23.
Segata, N., Izard, J., Waldron, L., Gevers, D., Miropolsky, L., Garrett, W.S., Huttenhower, C., 2011. Metagenomic biomarker discovery and explanation. Genome. Biol. 12, R60.
Sorokin, D.Y., Tourova, T., Mußmann, M., Muyzer, G., 2008. *Dethiobacter alkaliphilus gen. nov.sp. nov.*, and *Desulfurivibrio alkaliphilus gen. nov. sp. nov.*: two novel representatives of reductive sulfur cycle from soda lakes. Extremophiles 12, 431–439.
Sun, W., Cupples, A.M., 2012. Diversity of five anaerobic toluene-degrading microbial communities investigated using stable isotope probing. Appl. Environ. Microbiol. 78, 972–980.
Sun, W., Xie, S., Luo, C., Cupples, A.M., 2010. Direct link between toluene degradation in contaminated-site microcosms and a *Polaromonas strain*. Appl. Environ. Microbiol. 76, 956–959.
Sun, W., Sun, X., Cupples, A.M., 2014. Presence, diversity and enumeration of functional genes (*bssA* and *bamA*) relating to toluene degradation across a range of redox conditions and inoculum sources. Biodegradation 25, 189–203.
Sun, M., Xiao, T., Ning, Z., Xiao, E., Sun, W., 2015a. Microbial community analysis in rice paddy soils irrigated by acid mine drainage contaminated water. Appl. Microbiol. Biotechnol. 99, 2911–2922.
Sun, W., Li, Y., McGuinness, L.R., Luo, S., Huang, W., Kerkhof, L.J., Mack, E.E., Häggblom, M.M., Fennell, D.E., 2015b. Identification of anaerobic aniline-degrading bacteria at a contaminated industrial site. Environ. Sci. Technol. 49, 11079–11088.
Sun, W., Xiao, T., Sun, M., Dong, Y., Ning, Z., Xiao, E., Tang, S., Li, J., 2015c. Diversity of the sediment microbial community in the Aha watershed (Southwest China) in response to acid mine drainage pollution gradients. Appl. Environ. Microbiol. 81, 4874–4884.
Sun, W., Xiao, E., Dong, Y., Tang, S., Krumins, V., Ning, Z., Sun, M., Zhao, Y., Wu, S., Xiao, T., 2016. Profiling microbial community in a watershed heavily contaminated by an active antimony (Sb) mine in Southwest China. Sci. Total. Environ. 550, 297–308.
Tamura, H., Goto, K., Yotsuyan, T., Nagayama, M., 1974. Spectrophotometric determination of iron(II) with 1,10-Phenanthroline in presence of large amounts of iron(III). Talanta 21, 314–318.
Temple, K.L., Colmer, A.R., 1951. The autotrophic oxidation of iron by a new bacterium: *Thiobacillus ferrooxidans*. J. Bacteriol. 62, 605.
Terry, L.R., Kulp, T.R., Wiatrowski, H., Miller, L.G., Oremland, R.S., 2015. Microbiological oxidation of antimony (III) with oxygen or nitrate by bacteria isolated from contaminated mine sediments. Appl. Environ. Microbiol. 81, 8478–8488.
The Council of the European Communities, 1976. Council Directive 76/464/EEC of 4 May 1976 on Pollution Caused by Certain Dangerous Substances Discharged into the Aquatic Environment of the Community.
Tonomura, M., Ehara, A., Suzuki, H., Amachi, S., 2015. Draft genome sequence of *Anaeromyxobacter sp. strain PSR-1*, an arsenate-respiring bacterium isolated from arsenic-contaminated soil. Genomea A. 3 e00472–15.
Torma, A.E., Gabra, G.G., 1977. Oxidation of stibnite by*Thiobacillus ferrooxidans*. Ant. Leeuw. 43, 1–6.
Tucker, M., Barton, L., Thomson, B., 1998. Reduction of Cr, Mo, Se and U by *Desulfovibrio desulfuricans* immobilized in polyacrylamide gels. Ind. Microbiol. Biotechnol. 20, 13–19.
Ue, H., Matsuo, Y., Kasai, H., Yokota, A., 2011. *Demequina globuliformis sp. nov.*, *Demequina oxidasica sp. nov.* and *Demequina aurantiaca sp. nov.*, actinobacteria isolated from marine environments, and proposal of *Demequinaceae fam. nov.* Int. J. Syst. Evol. Microbiol. 61, 1322–1329.
USEPA, 1979. Water Related Fate of the 129 Priority Pollutants. USEPA, Washington, DC, USA.
Vasquez, L., Dagert, J.V.S., Scorza, J.V., Vicuna-Fernandez, N., de Pena, Y.P., Lopez, S., Bendezu, H., Rojas, E., Vasquez, L., Perez, B., 2006. Pharmacokinetics of experimental pentavalent antimony after intramuscular administration in adult volunteers. Curr. Ther. Res. Clin. Exp. 67, 193–203.
Waksman, S.A., Joffe, J., 1922. Microorganisms concerned in the oxidation of sulfur in the soil: II. *Thiobacillus thiooxidans*, a new sulfur-oxidizing organism isolated from the soil. J. Bacteriol. 7, 239.
Wang, Y., Qian, P.Y., 2009. Conservative fragments in bacterial 16S rRNA genes and primer design for 16S ribosomal DNA amplicons in metagenomic studies. PLoS One 4, e7401.
Weiss, J.V., Rentz, J.A., Plaia, T., Neubauer, S.C., Merrill-Floyd, M., Lilburn, T., Bradburne, C., Megonigal, J.P., Emerson, D., 2007. Characterization of Neutrophilic Fe (II)-Oxidizing bacteria isolated from the rhizosphere of wetland plants and description of Ferritrophicum radicicola gen. nov. sp. nov., and Sideroxydans paludicola sp. nov. Geomicrobiol. J. 24, 559–570.
Wenzel, W.W., Kirchbaumer, N., Prohaska, T., Stingeder, G., Lombi, E., Adriano, D.C., 2001. Arsenic fractionation in soils using an improved sequential extraction procedure. Anal. Chim. Acta 436, 309–323.
Wu, Q., Sanford, R.A., Löffler, F.E., 2006. Uranium (VI) reduction by Anaeromyxobacter dehalogenans strain 2CP-C. Appl. Environ. Microbiol. 72, 3608–3614.
Zhang, N., Wan, S., Li, L., Bi, J., Zhao, M., Ma, K., 2008. Impacts of urea N addition on soil microbial community in a semi-arid temperate steppe in northern China. Plant Soil 311, 19–28.